Supporting Information

Helical Assembly of a Dithienogermole Exhibiting Switchable Circularly Polarized Luminescence

Kyohei Hirano, Toshiaki Ikeda, Naoka Fujii, Takehiro Hirao, Masashi Nakamura, Yohei Adachi, Joji Ohshita, and Takeharu Haino*

Table of Contents

Experimental Section

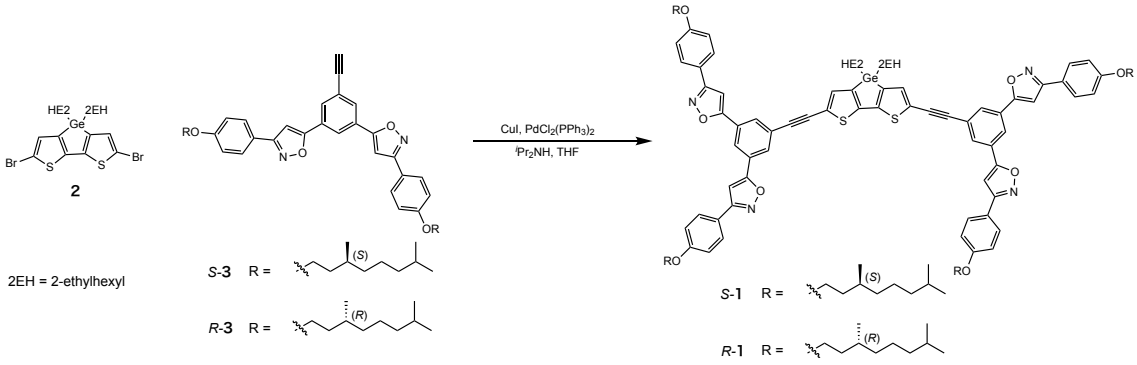

Scheme S1. Synthesis of *S*- and *R*-**1**.

General: All reagents and solvents were of the commercial reagent grade and were used without further purification except where noted. Dry CH_2Cl_2, DMF, and triethylamine were obtained by distillation over CaH_2. ^1H and ^{13}C NMR spectra were recorded on a Varian mercury-300 spectrometer at 25 °C in chloroform-*d* and chemical shifts were reported as the delta scale in ppm relative to $CHCl_3$ (δ = 7.260 for ^1H and 77.3 for ^{13}C). UV/vis absorption spectra were recorded on a JASCO V-560 spectrometer. Emission spectra were recorded on a JASCO FP-6500 spectrofluorometer. CD spectra were recorded on a JASCO J-1500 Circular Dichroism spectrometer. CPL spectra were recorded on a JASCO CPL-200 Circularly Polarized Luminescence spectrometer. ESI-Mass spectra were recorded on Thermo Scientific LTQ Orbitrap XL hybrid FTMS. AFM images were masured on a Keysight Technologies PicoView5100 microscope. Optical rotations were recorded on a JASCO DIP-370 polarimeter. UV/vis absorption, emission, CD, and CPL spectra in solution were measured using a conventional quartz cell (light path 1 cm) with temperature control. UV/vis absorption, emission, CD, and CPL spectra in gel phase were measured using a conventional quartz cell (light path 0.1 cm). Elemental analyses were performed using CHNS analyzer. Preparative separations were performed by silica gel gravity column chromatography (Silica Gel 60N (spherical, neutral)). Recycling preparative GPC-HPLC separations were carried out on JAI LC-908s using preparative JAIGEL-2H, 2H, 1H columns in series. Compounds **2**[1] and *S*- and *R*-**3**[2] were prepared according to reported methods.

Dithienogermole (*S*)-derivetive *S*-1: To a solution of **2** (237 mg, 0.381 mmol) and *S*-**3** (547 mg, 0.780 mmol) in THF (25 mL) was added diisopropylamine (1.0 mL) and CuI (4.0 mg, 0.021 mmol). The mixture was degassed by bubbling nitrogen for 30 min, and then $PdCl_2(PPh_3)_2$ (58.1 mg, 0.0828 mmol) was added to the mixture. The reaction mixture was refluxed in dark for 17 h. The reaction was quenched by addition of a portion of water. The organic layer was extracted with Et_2O, washed with

sat. NH_4Cl aq. and brine, dried over anhydrous Na_2SO_4, and concentrated in *vacuo*. The crude product was purified by column chromatography on silica gel (ethyl acetate/hexane 8%) to give the *S*-**1** as a yellow solid (112 mg, 16%). *S*-**1**: M.p. 80-81 ºC; $[\alpha]^{25}_D$ = –4.0 cm^3 g^{-1} dm^{-1} (c 0.01 g cm^{-3}); ^1H NMR (300 MHz, $CDCl_3$): δ 8.22 (t, 2H, *J* = 1.5 Hz), 8.02 (d, 4H, *J* = 1.5 Hz), 7.82 (d, 8H, *J* = 8.8 Hz), 7.34 (s, 2H), 7.01 (d, 8H, *J* = 8.8 Hz), 6.93 (s, 4H), 4.12-4.02 (m, 8H), 1.92-1.80 (m, 4H), 1.75-1.48 (m, 16H), 1.40-1.10 (m, 42H), 0.97 (d, 12H, *J* = 6.4 Hz), 0.88 (d, 24H, *J* = 6.4 Hz), and 0.84 (t, 12H, *J* = 7.3 Hz) ppm; ^{13}C NMR (75 MHz, $CDCl_3$): δ 168.2, 162.8, 160.7, 148.0, 146.1, 136.0, 129.2, 128.6, 128.2, 125.1, 123.1, 122.1, 120.9, 114.9, 98.5, 92.9, 85.7, 66.5, 39.3, 37.3, 37.0, 36.1, 35.5, 29.9, 28.9, 28.7, 28.0, 24.7, 23.0, 22.7, 22.6, 20.8, 19.7, 14.2, and 10.9 ppm; IR (ATR): ν 2952, 2924, 2870, 1610, 1563, 1524, 1460, 1435, 1384, 1363, 1295, 1248, 1173, 1115, 1055, 1016, 951, 912, 876, 833, 790, 761, and 647 cm^{-1}; HRMS (ESI^+): calcd for *m*/*z* 1861.9867 $[M+H]^+$, found *m*/*z* 1861.9940; Anal. calcd for $C_{116}H_{146}N_4O_8S_2Ge$: C 74.86, H 7.91, N 3.01, S 3.45, found C 74.73, H 7.78, N 2.97, S 3.30%.

Dithienogermole (*R*)-derivetive *R*-1: To a solution of **2** (144 mg, 0.232 mmol) and *S*-**3** (332 mg, 0.473 mmol) in THF (6 mL) was added diisopropylamine (0.5 mL) and CuI (6.9 mg, 0.036 mmol). The mixture was degassed by bubbling nitrogen for 30 min, and then $PdCl_2(PPh_3)_2$ (67.0 mg, 0.0955 mmol) was added to the mixture. The reaction mixture was refluxed in dark for 9 h. The reaction was quenched by addition of a portion of water. The organic layer was extracted with Et_2O, washed with sat. NH_4Cl aq. and brine, dried over anhydrous Na_2SO_4, and concentrated in *vacuo*. The crude product was purified by column chromatography on silica gel (ethyl acetate/hexane 8%) to give the *R*-**1** as a yellow solid (57 mg, 13 %). *R*-**1**: M.p. 79-80 ºC; $[\alpha]^{25}_D$ = 3.0 cm^3 g^{-1} dm^{-1} (c 0.01 g cm^{-3}); ^1H NMR (300 MHz, $CDCl_3$): δ 8.19 (t, 2H, *J* = 1.5 Hz), 8.00 (d, 4H, *J* = 1.5 Hz), 7.81 (d, 8H, *J* = 8.8 Hz), 7.34 (s, 2H), 7.00 (d, 8H, *J* = 8.8 Hz), 6.91 (s, 4H), 4.12-4.02 (m, 8H), 1.92-1.80 (m, 4H), 1.75-1.48 (m, 16H), 1.40-1.10 (m, 42H), 0.97 (d, 12H, *J* = 6.4 Hz), 0.88 (d, 24H, *J* = 6.4 Hz), and 0.85 (t, 12H, *J* = 7.3 Hz) ppm; ^{13}C NMR (75 MHz, $CDCl_3$): δ 168.2, 162.8, 160.7, 148.0, 146.1, 136.0, 129.3, 128.6, 128.2, 125.1, 123.1, 122.1, 120.9, 114.9, 98.5, 92.9, 85.7, 66.5, 39.2, 37.3, 37.0, 36.1, 35.5, 29.8, 28.9, 28.7, 28.0, 24.7, 23.0, 22.7, 22.6, 20.8, 19.7, 14.2, and 10.9 ppm; IR (ATR): ν 2957, 2924, 2865, 2192, 1611, 1567, 1526, 1460, 1434, 1386, 1294, 1247, 1173, 1114, 1052, 1015, 949, 916, 879, 831, 790, 765, 687, and 651 cm^{-1}; HRMS ($APCI^+$): calcd for *m*/*z* 1861.9867 $[M+H]^+$, found *m*/*z* 1861.9867; Anal. calcd for $C_{116}H_{146}N_4O_8S_2Ge$: C 74.86, H 7.91, N 3.01, S 3.45, found C 74.82, H 7.88, N 2.93, S 3.41%.

Analysis of isodesmic self-assembly by ^{1}H NMR experiments: Hyperbolic curves were obtained by plotting of compound concentrations vs ^{1}H NMR chemical shifts (δ) of the aromatic protons. The curve-fitting analysis of the plots was carried out on the basis of an isodesmic association model, which is a type of unlimited self-association where the addition of each successive monomer to polymer involves an equal association constant ($K_2 = K_3 = ... = K_n = K_i$).[3] The fitting functions are given by equation 1 for NMR experiments. δ denotes apparent chemical shifts obtained from spectra; δ_m and δ_a are chemical shifts for a monomer and self-assembled species, respectively. K_i is the association constant; and c is the total concentration of a compound. The complexation-induced shift $\Delta\delta$ displays the difference between δ_m and δ_a.

$$\delta(c) = \delta_m + (\delta_a - \delta_m)\left(1 + \frac{1-\sqrt{4K_i c+1}}{2K_i c}\right) \qquad (1)$$

Analysis of cooperative self-assembly by temperature-dependent CD spectra: Degree of aggregation (α_{agg}) were calculated from the following equation 2:

$$\alpha_{agg}(T) = \frac{\theta(T)}{\theta_a} \qquad (2)$$

where $\theta(T)$ is the measured molar ellipticity at the absolute temperature T; θ_a is the molar ellipticity of the fully aggregated state. The latter value could be determined from the data or were determined by extrapolation of the measured extinction coefficient to their asymptotic value at high and low temperature, respectively. Non-sigmoidal melting curves were obtained by plotting of $\alpha_{agg}(T)$ vs T. The curve-fitting analysis of the plots was carried out on the basis of van der Schoot mathematical model.[4]

In the elongation regime, $\alpha_{agg}(T)$ is given by the following equation 3:

$$\alpha_{agg}(T) = \alpha_{sat}\left(1 - \exp\left[\frac{-\Delta H_e}{RT_e^2}(T - T_e)\right]\right) \qquad (3)$$

where ΔH_e is the molecular enthalpy release due to noncovalent interactions during elongation, T_e is the elongation temperature and R is the gas constant. α_{sat} is introduced as a parameter to ensure that $\alpha_{agg}(T)/\alpha_{sat}$ does not exceed unity. At temperatures above the elongation temperature T_e (i.e., the nucleation regime) the fraction of aggregated molecules is described by equation 4:

$$\alpha_{agg}(T) = K_a^{\frac{1}{3}} \exp\left[\left(\frac{2}{3}K_a^{\frac{1}{3}} - 1\right)\frac{h_e}{RT_e^2}(T - T_e)\right] \qquad (4)$$

where K_a is the dimensionless equilibrium constant of the activation step at T_e. The average length of the stack, $\langle N_n(T_e)\rangle$, averaged over the nucleated species, at the elongation temperature is given by equation 5:

$$\langle N_n(T_e)\rangle = \frac{1}{K_a^{\frac{1}{3}}} \qquad (5)$$

Hence, a higher degree of cooperativity is expressed in a smaller K_a value and will lead to a larger nucleus before elongation sets in. In the elongation regime the number-averaged degree of polymerization, averaged over all active species, $\langle N_n\rangle$, is given by equation 6:

$$\langle N_n\rangle = \frac{1}{K_a^{\frac{1}{2}}} \frac{\alpha_n}{\alpha_{sat}-\alpha_n} \qquad (6)$$

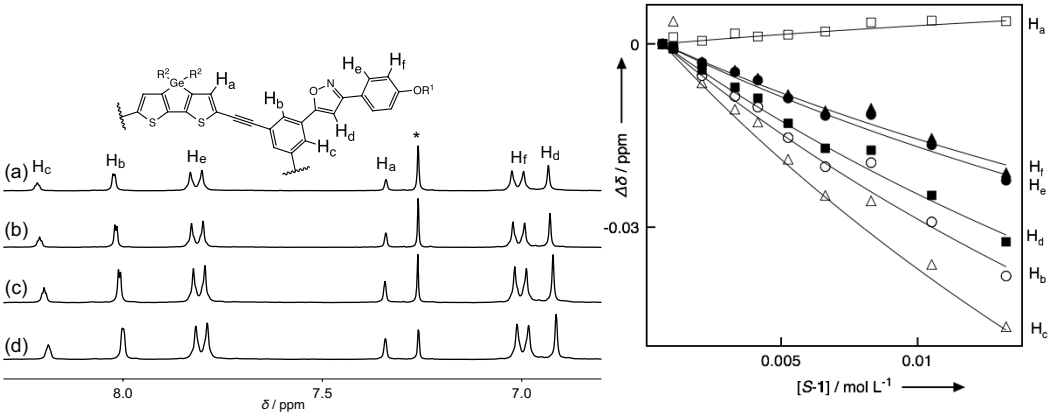

Figure S1. (left) Concentration-dependent ^{1}H NMR spectra of *S*-**1** in chloroform-*d* at 25 °C. The concentrations are (a) 5.3, (b) 6.6, (c) 10.5, and (d) 13.2 mmol L^{-1}. (right) Non-linear curve fitting of the self-assembly of *S*-**1** using ^{1}H NMR in chloroform-*d* at 25 ºC. The lines display fitting curves based on isodesmic model.

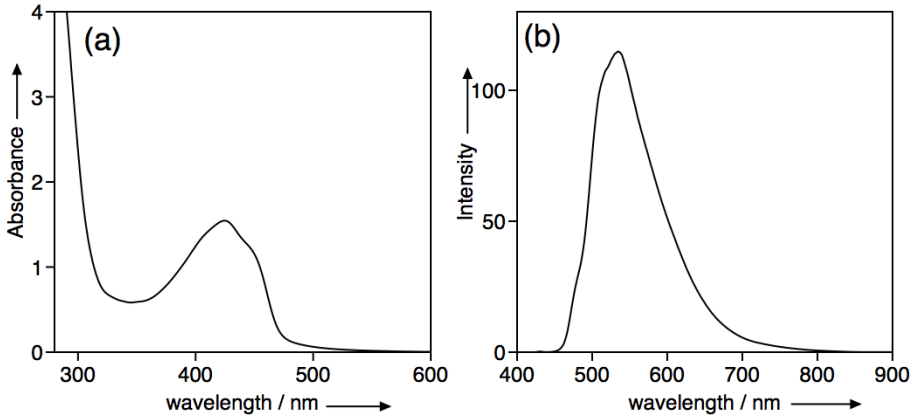

Figure S2. (a) UV-vis absorption and (b) emission spectra of *S*-**1** in chloroform at 25 ºC. [*S*-**1**] = 4.8 × 10^{-4} mol L^{-1}. λ_{ex} = 420 nm.

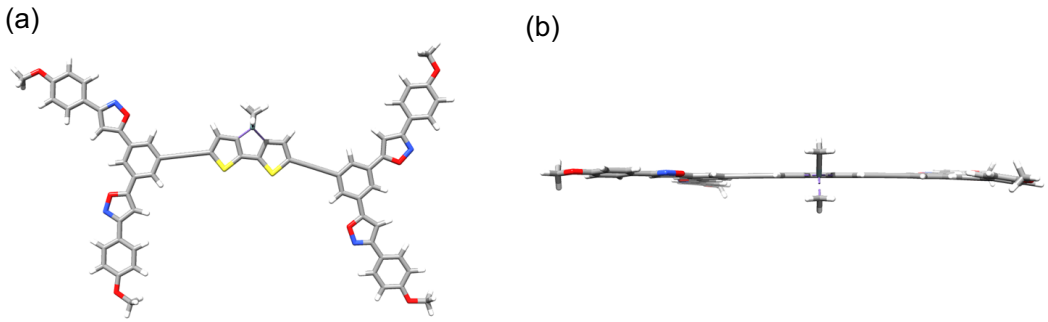

Figure S3. Energy minimized structure calculated by DFT method at B3LYP/6-31G(d) level[5] of methyl-substituted analogue of *S*-**1**. (a) Top view and (b) side view.

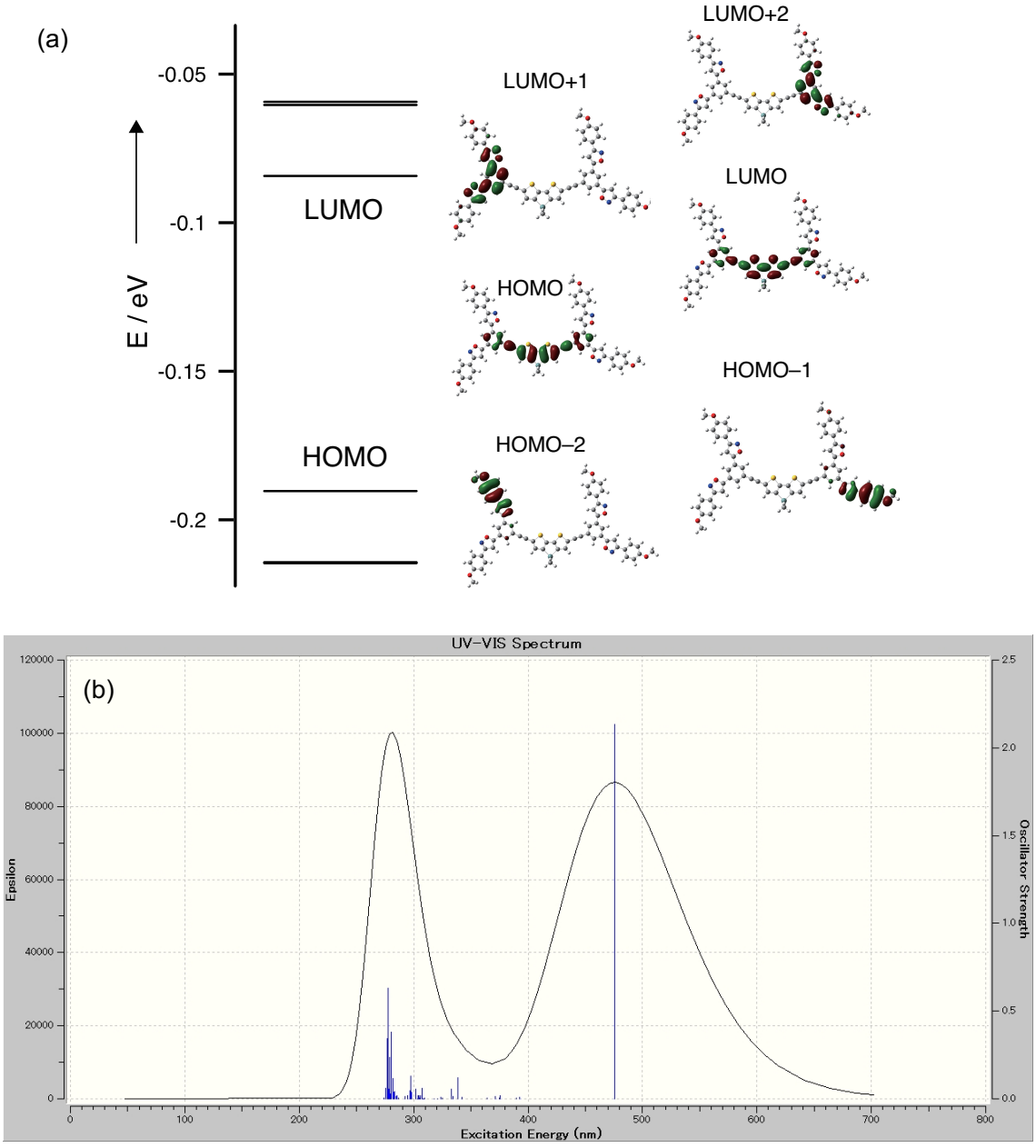

Figure S4. (a) Energy diagram of methyl-substituted analogue of *S*-**1** calculated by TD-DFT at B3LYP/6-31G(d) level. (b) Calculated UV/vis absorption spectrum.

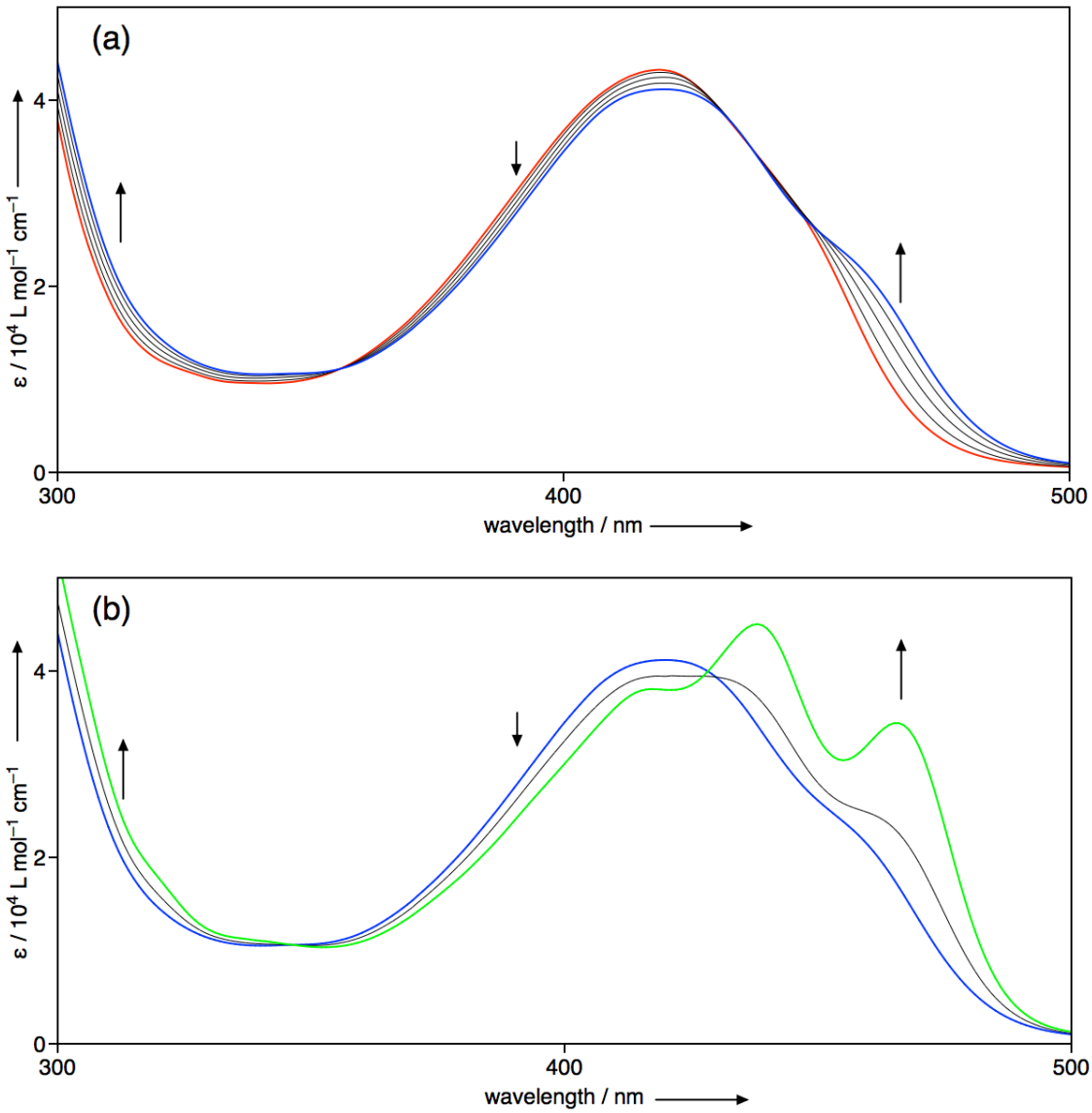

Figure S5. Temperature-dependent UV-vis absorption spectra of *S*-**1** in MCH. The spectra were recorded every 10 °C. The arrows indicate the change in the spectra as the temperature decrease from (a) 50 to 10 and (b) 10 to –10 °C. Red, blue, and green lines display the spectra at 50, 10, and –10 °C, respectively. [**1**] = 1.5×10^{-4} mol L^{-1}.

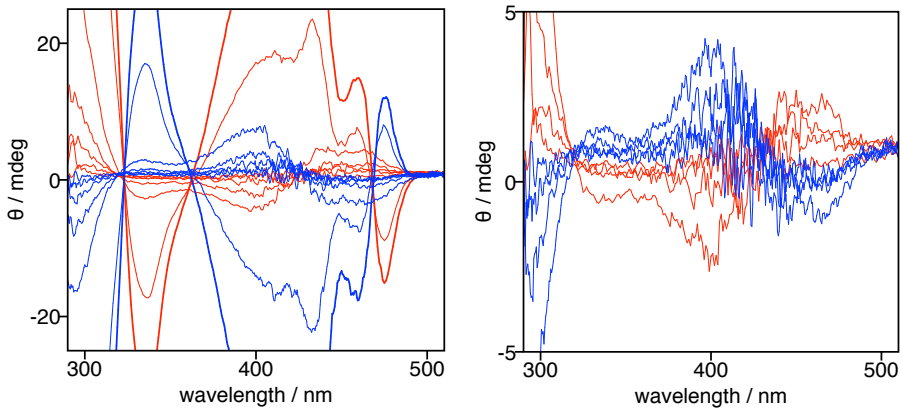

Figure S6. Temperature-dependent CD spectra of (red) *S*-**1** and (blue) *R*-**1** in MCH (a) at 50, 40, 30, 20, 10, 0, –10 °C and (b) at 50, 40, 30, 20 °C in the expanded window. [*S*-**1**] = [*R*-**1**] = 4.9 × 10^{-4} mol L^{-1}.

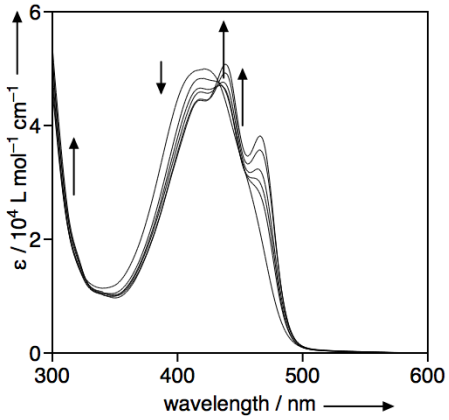

Figure S7. Concentration-dependent UV-vis absorption spectra of *S*-**1** in MCH at 0 ºC. The concentrations are 47, 33, 19, 14, 9, and 5 × 10^{-5} mol L^{-1}. The arrows indicate the change in the spectra as the concentration increase.

Note 1: The concentration-dependent UV-vis absorption spectra of *S*-**1** in MCH at 0 °C exhibited a spectral change similar to temperature-dependent one (Figure S5). At low concentration ([*S*-**1**] = 5.0 × 10^{-5} mol L^{-1}), monomeric absorption was observed at 423 nm, whereas absorption bands of the assembly appeared at 438 and 466 nm as the concentration increased up to 4.9 × 10^{-4} mol L^{-1}, indicating the formation of the assembly in the concentrated situation.

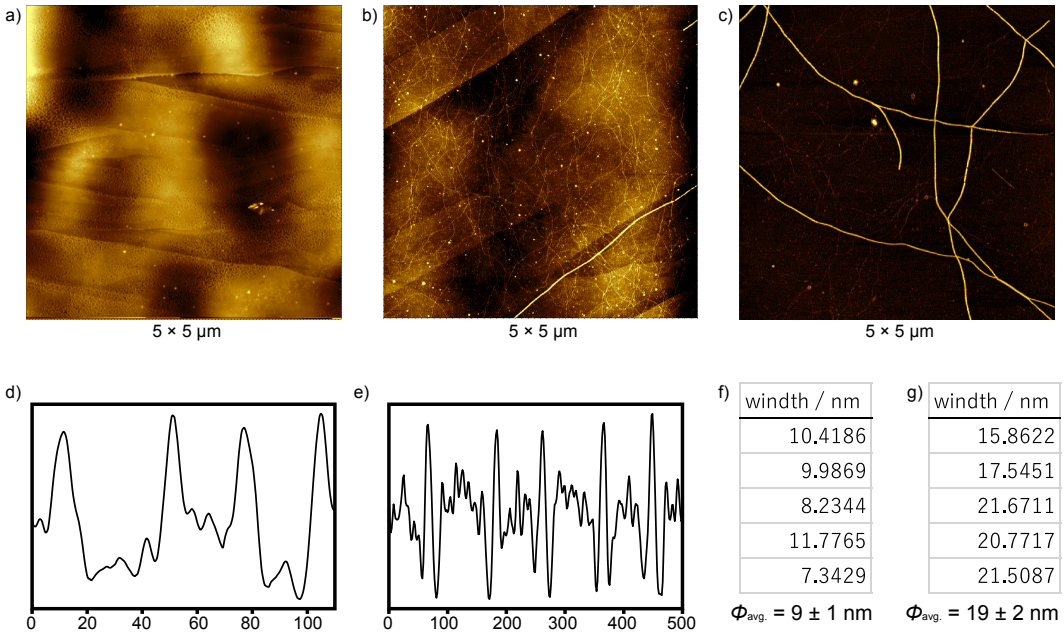

f)

width / nm
10.4186
9.9869
8.2344
11.7765
7.3429

$\Phi_{avg.}$ = 9 ± 1 nm

g)

width / nm
15.8622
17.5451
21.6711
20.7717
21.5087

$\Phi_{avg.}$ = 19 ± 2 nm

Figure S8. (a–c): AFM images of spin-coated thin films prepared from the solution of S-1 (4.9×10^{-4} mol L^{-1}) at (a) 50, (b) 10 and (c) –15 °C. (d, e): The phase profiles of the images (b) and (c) obtained from images (b) and (c). (f,g) The width values of the profiles obtained from images (b) and (c).

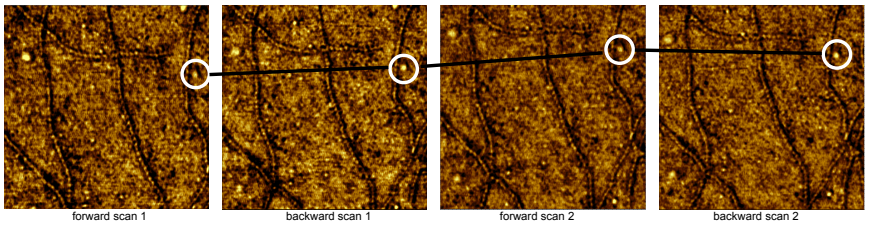

pitch / nm	pitch / nm
12.0303	12.3045
12.0305	10.1952
14.5072	11.3288
12.3842	14.508
8.492	7.0874
15.5688	11.6828
8.1367	11.6828
11.9531	11.3288
10.1952	12.0368
9.8437	7.4345

Averaged pitch: 11 ± 2 nm

Figure S9. A series of four consecutive scan AFM images (500 × 500 nm) of the thin film prepared from the solution of *S*-**1** (4.9×10^{-4} mol L^{-1}) at 10 °C. The pitch values of the helix obtained from the images are summarized in a table (right). The right-handed helical sense is maintained in all the images.

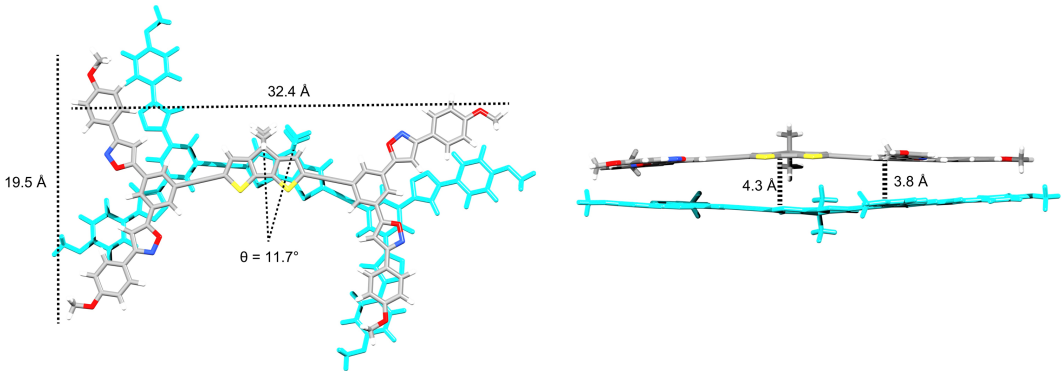

Figure S10. Calculated structure of the stacked dimer of **1** without the long alkyl chains. The calculation was carried out by Macromodel V9.1 using MMFFs force field.

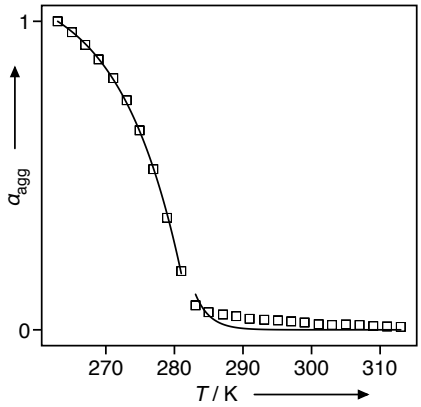

Figure S11. Plot of the degree of aggregation (α_{agg}) at 300 nm of *S*-**1** in MCH vs temperature. [*S*-**1**] = 4.9 ×10^{-4} mol L^{-1}. A Curve shows the fitting curve based on van der Schoot's model.

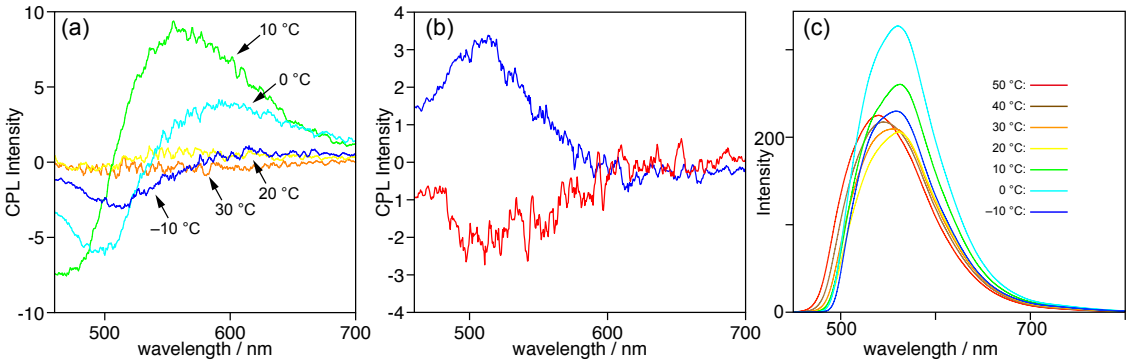

Figure S12. (a) Temperature-dependent CPL spectra of *S*-**1** in MCH. The temperatures are (orange) 30, (yellow) 20, (green) 10, (cyan) 0, and (blue) –10 ºC. (b) CPL spectra of (red) *S*-**1** and (blue) *R*-**1** in MCH at –10 ºC. (c) Temperature-dependent emission spectra of *S*-**1** in MCH. [*S*-**1**] = [*R*-**1**] = 4.9 × 10^{-4} mol L^{-1}. λ_{ex} = 420 nm.

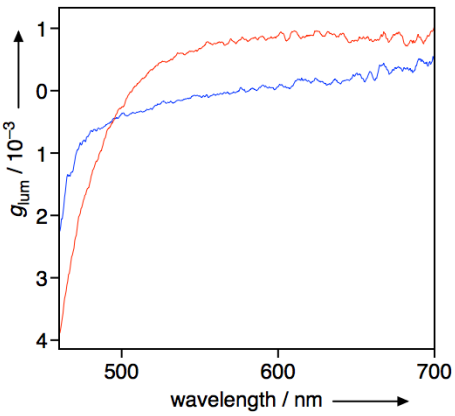

Figure S13. Plots of g_{lum} of *S*-**1** vs wavelength in MCH. The temperatures are (red) 10 ºC and (blue) –10 ºC, respectively. [*S*-**1**] = 4.9 × 10^{-4} mol L^{-1}.

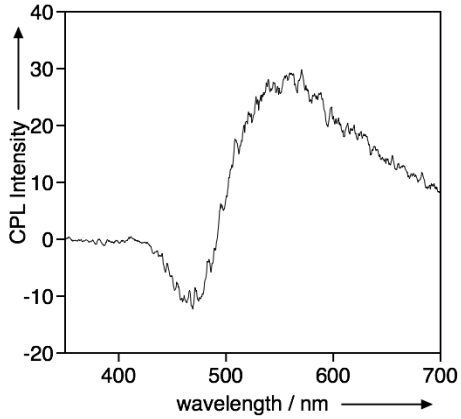

Figure S14. CPL spectra of *S*-**1** in MCH at 0 ºC. [*S*-**1**] = 4.9×10^{-4} mol L^{-1}. λ_{ex} = 260 nm.

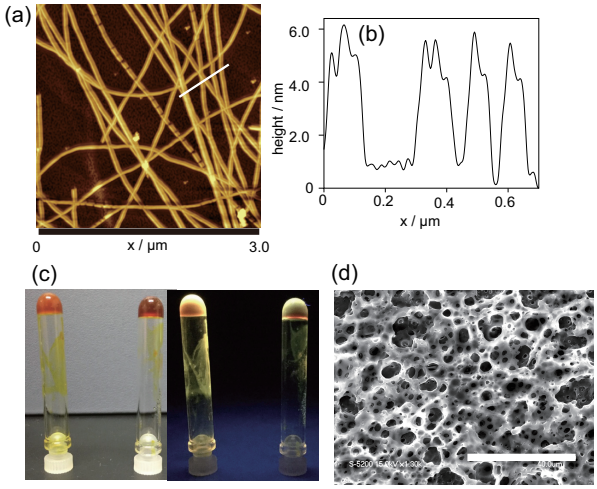

Figure S15. (a) The AFM image of *S*-**1** on HOPG plate. (b) The height profile of the white line in (a). (c) Photographs of organogels of *S*-**1** (left) under daylight and (right) under UV light. The solvents are (left) hexane and (right) cyclohexane. (d) The FE-SEM image of the xerogel of *S*-**1**. Scale bar displays 40 µm.

Table S1. Gelation properties of *S*-**1**.[a],[b],[c]

solvent		solvent	
hexane	G (39)	acetone	P
methylcyclohexane	G (12)	2-butanone	S
cyclohexane	G (9.8)	ethyl acetate	S
heptane	G (41)	diethyl ether	S
2-methyl-2-butene	G (78)	1,4-dioxane	S
1-butanol	G (25)	dichloromethane	S
benzene	S	acetonitrile	I
toluene	S	ethanol	I
cyclohexene	S	2-propanol	I
pyridine	S	2-propyn-1-ol	I

[a] G = gel, P = precipitation, S = solution, and I = insoluble. [b] P, I, and S are at [**1**] = 20 g L^{-1}. [c] The critical gelation concentration (g L^{-1}) is shown in parentheses.

References

[1] J. Ohshita, Y.-M. Hwang, T. Mizumo, H. Yoshida, Y. Ooyama, Y. Harima, Y. Kunugi, *Organometallics* 2011, **30**, 3233.

[2] T. Ikeda, M. Takayama, J. Kumar, T. Kawai, T. Haino, *Dalton Trans.* 2015, **44**, 13156.

[3] *Supramolecular Polymers, 2nd ed.*; Ciferri, A., Ed.; CRC Press - Taylor & Francis: Boca Raton, FL, 2005.

[4] M. M. J. Smulders, A. P. H. J. Schenning and E. W. Meijer, *J. Am. Chem. Soc.*, 2008, **130**, 606.

[5] M. J. Frisch, G. W. Trucks, H. B. Schlegel, G. E. Scuseria, M. A. Robb, J. R. Cheeseman, G. Scalmani, V. Barone, B. Mennucci, G. A. Petersson, H. Nakatsuji, M. Caricato, X. Li, H. P. Hratchian, A. F. Izmaylov, J. Bloino, G. Zheng, J. L. Sonnenberg, M. Hada, M. Ehara, K. Toyota, R. Fukuda, J. Hasegawa, M. Ishida, T. Nakajima, Y. Honda, O. Kitao, H. Nakai, T. Vreven, J. A. Montgomery, Jr., J. E. Peralta, F. Ogliaro, M. Bearpark, J. J. Heyd, E. Brothers, K. N. Kudin, V. N. Staroverov, R. Kobayashi, J. Normand, K. Raghavachari, A. Rendell, J. C. Burant, S. S. Iyengar, J. Tomasi, M. Cossi, N. Rega, N. J. Millam, M. Klene, J. E. Knox, J. B. Cross, V. Bakken, C. Adamo, J. Jaramillo, R. Gomperts, R. E. Stratmann, O. Yazyev, A. J. Austin, R. Cammi, C. Pomelli, J. W. Ochterski, R. L. Martin, K. Morokuma, V. G. Zakrzewski, G. A. Voth, P. Salvador, J. J. Dannenberg, S. Dapprich, A. D. Daniels, Ö. Farkas, J. B. Foresman, J. V. Ortiz, J. Cioslowski and D. J. Fox, Gaussian, Inc., Wallingford CT, 2010.

^{1}H and ^{13}C NMR spectra of *S*-**1**.

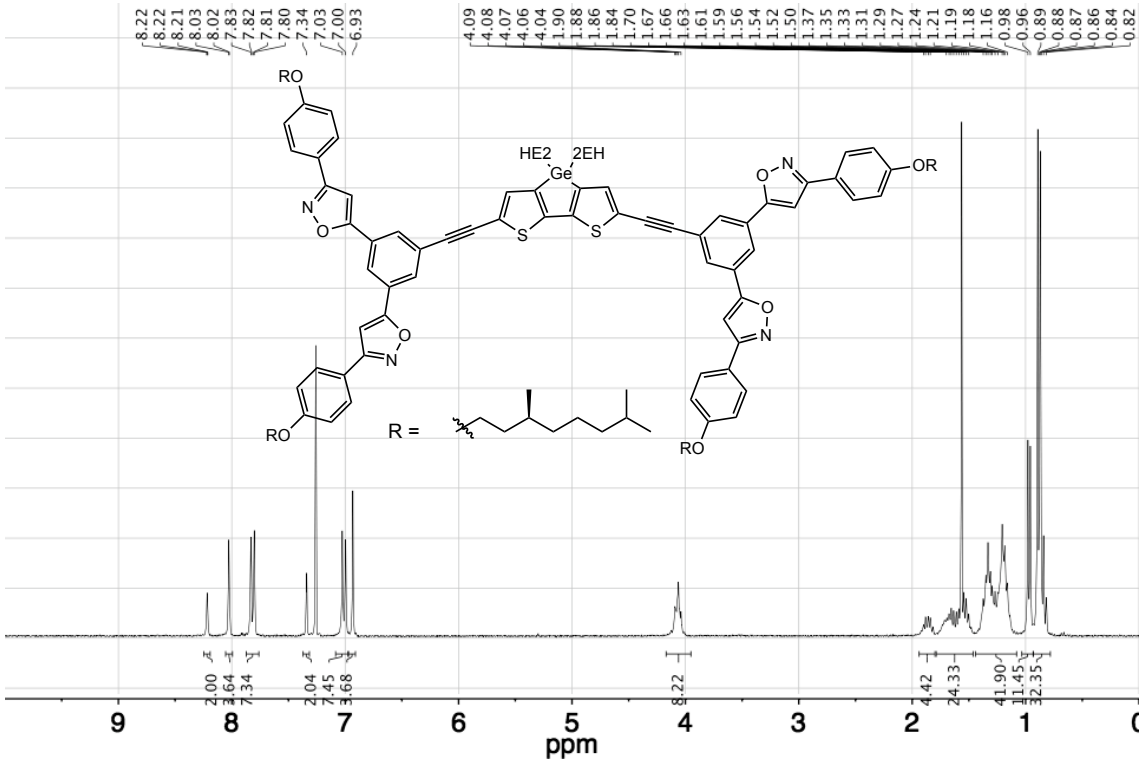

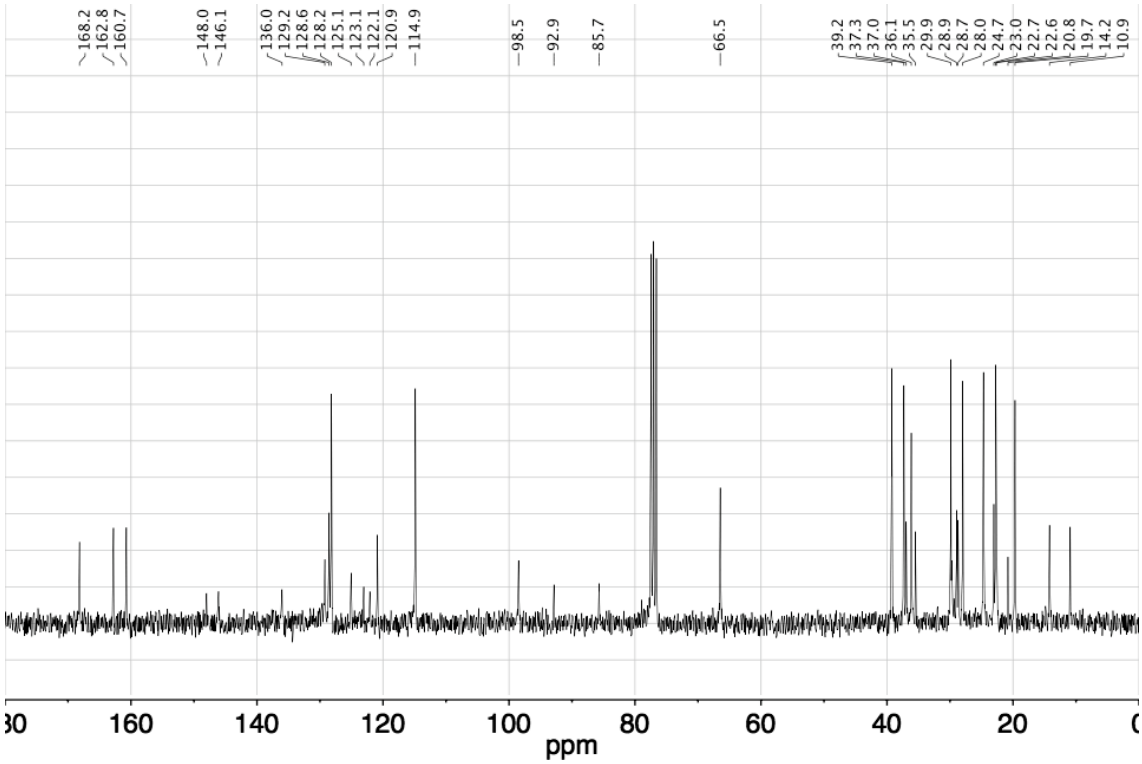

^{1}H and ^{13}C NMR spectra of *R*-**1.**

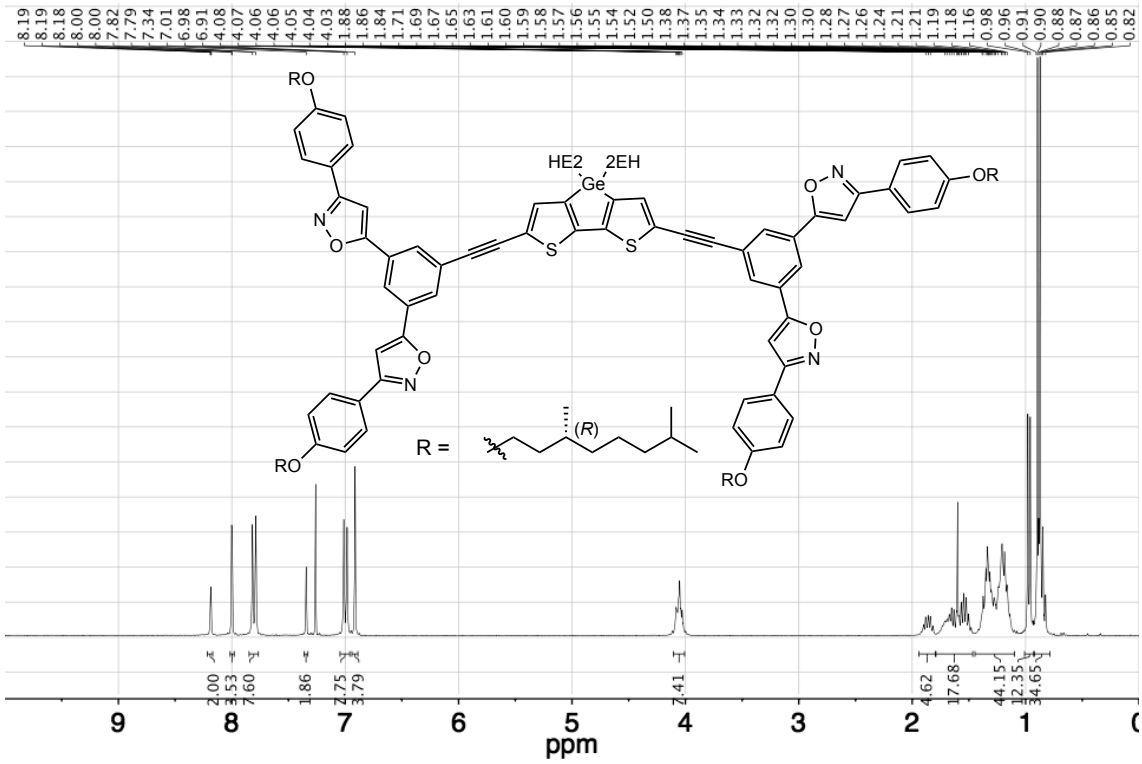

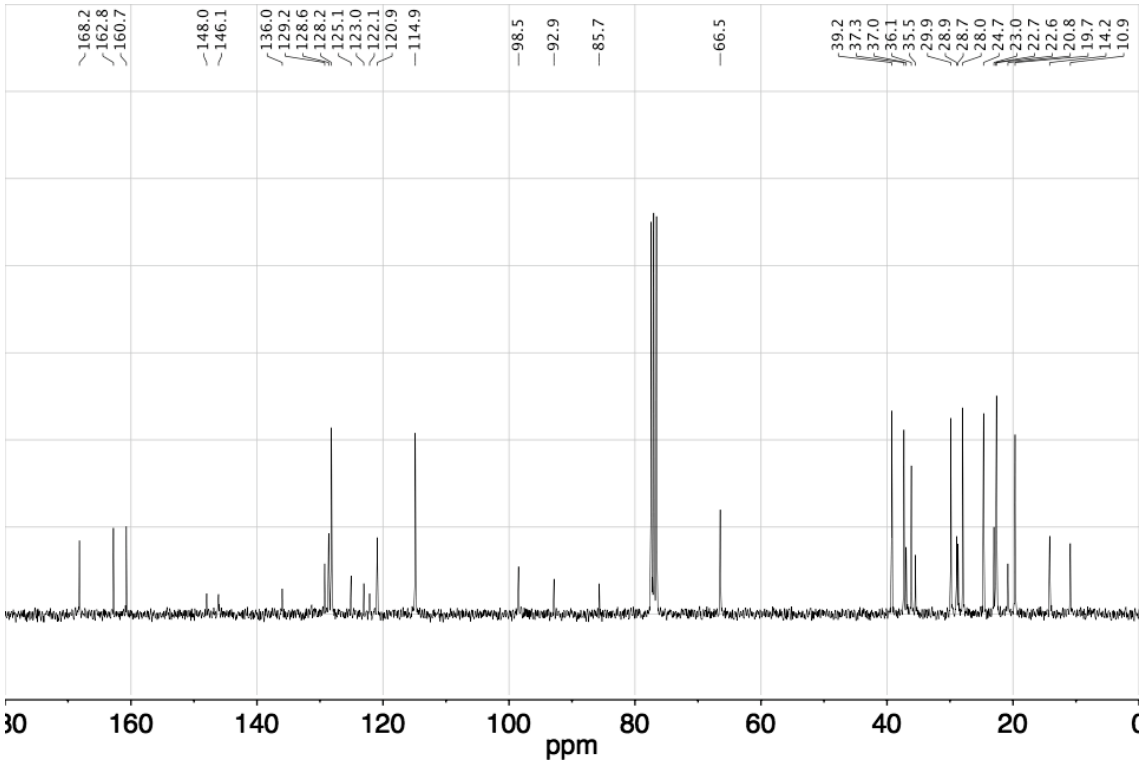

Calculated Structure of methyl-substituted analogue of *S*-**1.**

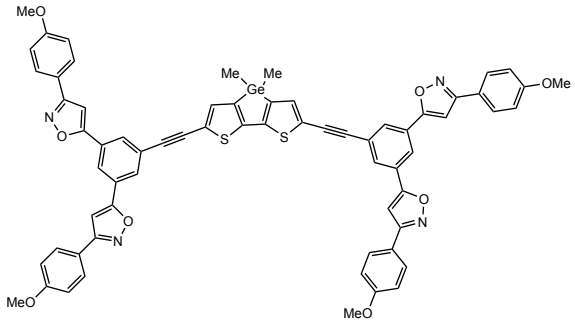

Framework group C1[X(C66H46GeN4O8S2)]

Deg. of freedom 375

Standard orientation:

Center Number	Atomic Number	Atomic Type	Coordinates (Angstroms) X	Y	Z
1	6	0	1.480998	-3.386311	-0.036833
2	6	0	0.832564	-2.153372	-0.035807
3	6	0	-0.613790	-2.152221	-0.038967
4	6	0	-1.264005	-3.384494	-0.042422
5	32	0	0.107888	-4.769879	-0.042820
6	16	0	-1.721889	-0.815224	-0.038112
7	6	0	-2.666626	-3.242696	-0.043980
8	6	0	-3.099544	-1.922814	-0.041897
9	16	0	1.943559	-0.818380	-0.029422
10	6	0	3.319084	-1.928781	-0.027869
11	6	0	2.884002	-3.247798	-0.032420
12	6	0	-5.544772	-0.981534	-0.039427
13	6	0	-4.412175	-1.431625	-0.041185
14	6	0	5.771592	-1.006883	-0.015867
15	6	0	4.633524	-1.442691	-0.021779
16	6	0	-9.484847	0.550947	-0.022789
17	6	0	-8.395722	1.433538	-0.043882
18	6	0	-7.092046	0.923515	-0.050765
19	6	0	-6.870172	-0.466386	-0.035295

20	6	0	-7.972551	-1.338610	-0.013466
21	6	0	-9.279363	-0.834991	-0.007468
22	6	0	9.735363	0.462638	0.007514
23	6	0	9.506893	-0.920717	-0.001113
24	6	0	8.193648	-1.405297	-0.009040
25	6	0	7.105070	-0.513110	-0.008245
26	6	0	7.350109	0.871114	0.000541
27	6	0	8.661531	1.362703	0.008441
28	6	0	-10.422346	-1.748389	0.013705
29	6	0	-10.546694	-3.108714	0.018582
30	6	0	-11.956083	-3.341489	0.041805
31	7	0	-12.622306	-2.198916	0.050112
32	8	0	-11.657558	-1.192955	0.032473
33	6	0	-8.625403	2.878548	-0.057888
34	6	0	-9.748759	3.654567	-0.017604
35	6	0	-9.260041	4.996124	-0.061953
36	7	0	-7.938806	5.014718	-0.123562
37	8	0	-7.536087	3.680506	-0.121727
38	6	0	8.907660	2.805034	0.017760
39	6	0	8.094054	3.902071	0.022603
40	6	0	8.990082	5.014800	0.031832
41	7	0	10.248336	4.606753	0.032366
42	8	0	10.199041	3.213340	0.023516
43	6	0	10.638068	-1.848829	-0.001570
44	6	0	11.993599	-1.681636	0.006740
45	6	0	12.519372	-3.009848	0.000807
46	7	0	11.543774	-3.903080	-0.010369
47	8	0	10.356011	-3.173385	-0.011814
48	6	0	-14.065579	-7.075573	0.081851
49	6	0	-14.768461	-5.858866	0.087378
50	6	0	-14.083905	-4.655898	0.074465
51	6	0	-12.675450	-4.624559	0.055582
52	6	0	-11.988432	-5.842712	0.050323

53	6	0	-12.666356	-7.063028	0.063142
54	6	0	-11.479162	8.665809	-0.016034
55	6	0	-10.078700	8.680563	-0.129335
56	6	0	-9.365858	7.494044	-0.144314
57	6	0	-10.024844	6.252610	-0.047031
58	6	0	-11.418959	6.252346	0.065218
59	6	0	-12.149878	7.441574	0.081475
60	6	0	8.066548	9.203067	0.056489
61	6	0	9.402455	8.767383	0.060298
62	6	0	9.696875	7.414794	0.052365
63	6	0	8.669809	6.450407	0.040285
64	6	0	7.344700	6.897893	0.036587
65	6	0	7.033921	8.258736	0.044571
66	6	0	16.618960	-4.269087	0.015208
67	6	0	15.582126	-5.217390	0.011873
68	6	0	14.259812	-4.807696	0.007319
69	6	0	13.926416	-3.438813	0.005857
70	6	0	14.968272	-2.505689	0.009148
71	6	0	16.305717	-2.905213	0.013826
72	8	0	-14.832943	-8.200687	0.095649
73	8	0	-12.084186	9.886289	-0.010875
74	8	0	7.885405	10.552833	0.065020
75	8	0	17.883478	-4.775775	0.019675
76	6	0	-14.181655	-9.461957	0.090816
77	6	0	-13.498220	9.937797	0.103799
78	6	0	6.557715	11.055909	0.062306
79	6	0	18.973585	-3.866478	0.023469
80	6	0	0.110568	-5.873709	-1.645779
81	6	0	0.104320	-5.880800	1.555243
82	1	0	-3.370139	-4.068252	-0.046414
83	1	0	3.586397	-4.074215	-0.032148
84	1	0	-10.498901	0.932989	-0.020251
85	1	0	-6.246124	1.600385	-0.067005

86	1	0	-7.795919	-2.408647	-0.000469
87	1	0	10.747545	0.849676	0.013522
88	1	0	8.010969	-2.473209	-0.015711
89	1	0	6.507239	1.553706	0.001147
90	1	0	-9.754407	-3.840688	0.006109
91	1	0	-10.774093	3.323488	0.035501
92	1	0	7.015492	3.919729	0.020401
93	1	0	12.540507	-0.751835	0.016575
94	1	0	-15.853403	-5.888311	0.101836
95	1	0	-14.631882	-3.719552	0.078715
96	1	0	-10.902374	-5.855023	0.036146
97	1	0	-12.097954	-7.985867	0.058503
98	1	0	-9.575833	9.639561	-0.204697
99	1	0	-8.284634	7.511259	-0.232256
100	1	0	-11.958577	5.313069	0.144845
101	1	0	-13.229173	7.399556	0.170413
102	1	0	10.190155	9.514131	0.069626
103	1	0	10.730269	7.084347	0.055471
104	1	0	6.527892	6.182014	0.027162
105	1	0	5.994451	8.565438	0.041333
106	1	0	15.844471	-6.270679	0.013122
107	1	0	13.463255	-5.544324	0.004922
108	1	0	14.746813	-1.442378	0.007648
109	1	0	17.084544	-2.151511	0.016172
110	1	0	-14.977168	-10.208940	0.103825
111	1	0	-13.571810	-9.596954	-0.812072
112	1	0	-13.547763	-9.591365	0.977816
113	1	0	-13.760657	10.997033	0.088435
114	1	0	-13.989694	9.430026	-0.736466
115	1	0	-13.842594	9.492177	1.046245
116	1	0	6.650524	12.143249	0.070581
117	1	0	6.010973	10.745127	-0.837559
118	1	0	6.002465	10.732225	0.952355

119	1	0	19.875347	-4.481202	0.026766
120	1	0	18.970901	-3.230613	-0.871547
121	1	0	18.964500	-3.230402	0.918293
122	1	0	-0.776144	-6.515545	-1.659397
123	1	0	0.111231	-5.253296	-2.545299
124	1	0	0.998726	-6.513519	-1.657012
125	1	0	-0.782608	-6.522440	1.562790
126	1	0	0.992255	-6.520913	1.566952
127	1	0	0.101851	-5.264330	2.457468

Rotational constants (GHZ): 0.0170264 0.0045679 0.0036064